



## Improving the attrition resistance of slurry phase heterogeneous catalysts

Hien N. Pham <sup>a</sup>, Alexander Viergutz <sup>a,1</sup>, Robert J. Gormley <sup>b</sup>, Abhaya K. Datye <sup>a,\*</sup>

<sup>a</sup> Department of Chemical and Nuclear Engineering, Center for Microengineered Materials, University of New Mexico, Albuquerque, NM 87131-1341, USA

<sup>b</sup> Federal Energy Technology Center, Pittsburgh, PA 15236, USA

Received 18 November 1998; received in revised form 18 October 1999; accepted 25 October 1999

### Abstract

Slurry phase heterogeneous catalysts for processes such as Fischer–Tropsch (F–T) synthesis must exhibit a high degree of attrition resistance. The precipitated Fe–Cu catalyst used for F–T synthesis is quite weak in its as-prepared state. Spray-drying yields spherical particles which show some improvement in attrition resistance. However, the formation of fines ( $< 5 \mu\text{m}$ ) in this powder shows that it is not suitable as a slurry phase catalyst. In this paper, we report on the use of a silica binder to improve the strength of spray-dried agglomerates. The attrition resistance was measured using ultrasonic fragmentation followed by sedimentation particle size analysis. The attrition strength of the iron oxide catalyst agglomerates was compared to that of a commercial alumina powder, which was used as a reference material. The role of calcination (before or after spray-drying) and the method of silica binder addition (before or after spray-drying) was investigated. © 2000 Elsevier Science S.A. All rights reserved.

**Keywords:** Attrition resistance; Slurry phase heterogeneous catalysts; Fischer–Tropsch; Precipitated Fe–Cu catalyst

### 1. Introduction

This work is directed towards synthesis of iron oxide catalysts for Fischer–Tropsch (F–T) synthesis, a reaction that allows conversion of coal or natural gas into liquid fuels. For coal conversion, Fe catalysts are preferred since they can operate at the lower  $\text{H}_2/\text{CO}$  ratio in coal-derived syngas. These iron oxide catalysts are prepared by co-precipitation of iron and copper salts. Potassium is used as a promoter to improve catalyst selectivity. The preferred reactor type is a slurry phase bubble column which requires spherical catalyst agglomerates 50–70  $\mu\text{m}$  in diameter. Since the products of F–T synthesis are liquid hydrocarbon waxes, separation of product from the catalyst requires that the catalyst agglomerates be attrition-resistant.

In a previous study [1], we reported a comparison of two approaches used for measuring the attrition strength of catalyst agglomerates. Ultrasonic fragmentation coupled with particle size distribution measurements was found to

be more sensitive to differences in catalyst strength than the conventional approach involving uniaxial compaction. Recently, Oukaci et al. [2] compared cobalt-based F–T catalysts for their attrition using jet cup, ultrasound and slurry bubble column tests. They showed that, within experimental error, the relative attrition behavior of all three tests matched well amongst each other. The ultrasonic fragmentation technique, working with small sample size, can actually give a very good indication of attrition resistance.

Using the ultrasonic fragmentation approach [3,4], we were able to show that a plate-like kaolin binder did not impart any additional strength to a precipitated iron catalyst, that was otherwise weak and easily susceptible to attrition. As revealed by transmission electron microscopy (TEM), the kaolin and Fe F–T catalyst occurred as two distinct phases which, due to their plate-like structure, did not connect to create strong interlocking forces between them.

We have therefore explored the role of other binder morphologies to provide improved attrition resistance for Fe F–T catalysts. We have worked with silica because it is the preferred choice as a support for obtaining better product selectivity and activity in F–T synthesis. We report here a study of factors that determine the strength of

\* Corresponding author. Tel.: +1-505-277-0477; fax: +1-505-277-1024; e-mail: datye@unm.edu

<sup>1</sup> NSF/REU Summer Student, Department of Chemical Engineering, Cornell University, Ithaca, NY 14853, USA.

spray-dried agglomerates. When agglomerates are formed, binders are often used for the process. Binders play several roles, such as in controlling the release of drugs via a coating process, or in strengthening brittle materials. For example, Nikolic and Radonjic [5] used a sol-gel silica coating [6] to strengthen an alumina substrate. Bergna [7] prepared attrition-resistant porous particles by spray-drying slurries made of mixtures of micron-sized particles and discrete nanoparticles. These nanoparticles migrated to the periphery of the spray droplets where they coalesced to form a shell.

Several factors can have an effect on the strengths of agglomerates. Horisawa et al. [8] found that for their sample powders with polymer binders, the surface polarities of both powders and binders, as well as the degree of polymerization of the binder were important factors in determining the strength of granules. Bortzmeyer and Goimard [9] investigated three different  $\text{CaCO}_3$  powders and found that no correlation was observed between the attrition rate and the mechanical properties (tensile strength, fracture energy, etc.). However, a correlation between attrition rate and surface roughness was observed. The factors we have explored in this study include the method of silica addition, and the effect of calcination on the strength of spray-dried agglomerates prepared from precipitated iron oxide.

## 2. Experimental

A precipitated Fe–Cu catalyst (64.80% Fe, 6.24% Cu by ICP based on dried weight) in its wet form (labeled PRFECU-ED20-124) was used for the experiments. The starting materials were the nitrates of Fe and Cu, and  $\text{NH}_4\text{OH}$ . Solutions of Fe–Cu nitrate and  $\text{NH}_4\text{OH}$  were mixed at  $80^\circ\text{C}$  in a continuous flow through mixer, causing the iron oxide to precipitate out. The product catalyst was discarded until the pH was between 6.8 and 7.2. The catalyst was then collected in a filter funnel, and the filter cake was pumped down to being wet but not cracked. Samples of the filtrate were obtained; a pH and brown ring test were performed for each sample to ensure that the pH remained near 7.0 and that traces of nitrate ions were removed from the catalyst, respectively. The cake was removed and then resuspended in hot water. After filtering the slurry, samples of the filtrate were obtained for pH and brown ring testings. After the brown ring test was negative, the filter cake was pumped moist. Finally, once the precipitated Fe–Cu catalyst was dry enough to remove it off the filter, the catalyst was suspended in deionized  $\text{H}_2\text{O}$ .

In a typical run, 100 ml of the precipitated Fe–Cu catalyst was ultrasonicated at an amplitude of 20 for 2 min to break up any loose agglomerates. A Tekmar 501 ultrasonic disrupter (20 kHz  $\pm$  50 Hz) equipped with a V1A horn and a 1/2-in. probe tip was used for the ultrasonication process. The sample was then mixed with 11 ml of

potassium silicate solution (KASIL<sup>®</sup> #1; PQ), to obtain a silica loading of 25 wt.%. Dilute nitric acid (0.1 N; J.T. Baker) was added dropwise while the slurry was stirred until the pH was about 7. Deionized water was added to prepare 250 ml of slurry, and the mixture was stirred for  $\approx$  10 min. A Buchi 190 mini spray dryer was used to spray-dry the slurry.

The mini spray dryer made it easier to test several compositions in small batch sizes. The inlet temperature of the spray dryer was over  $200^\circ\text{C}$  with the outlet being maintained over  $100^\circ\text{C}$ . The powder was collected in a cyclone trap and then analyzed using a Sedigraph 5100 particle size analyzer and scanning electron microscope (SEM).

In another run, 200 ml of PRFECU-ED20-124 was ultrasonicated at an amplitude of 20 for 2 min. Deionized water was then added to prepare 250 ml of slurry. The slurry was spray-dried, and the dried Fe-based catalyst was collected in a cyclone trap. The sample was then mixed with 11 ml of potassium silicate solution and deionized water to prepare 250 ml of slurry, and the final mixture was spray-dried.

Other runs involved performing the procedure where a slurry of precipitated Fe–Cu catalyst and potassium silicate was spray-dried, followed by calcining the sample at  $300^\circ\text{C}$  for 2 h to see if there was any additional strength imparted to the sample, or calcining the  $\text{SiO}_2$ -containing catalyst first followed by adding deionized water to prepare 250 ml of slurry, and then spray-drying the slurry to see if there was any additional strength imparted to the sample. The  $\text{SiO}_2$ -containing catalyst was prepared by first mixing precipitated Fe–Cu catalyst with potassium silicate solution and adjusting the pH to 7. The mixture was filtered using a Buchner funnel to form a wet cake. The cake was dried overnight, and the dried product was ground to form a powder.

Our synthesized precipitated Fe–T catalysts were then compared to a VISTA alumina powder (VISTA-B-965-500C). The starting alumina from VISTA was sieved and calcined in air at  $500^\circ\text{C}$ . While this alumina is not prepared by spray-drying, it is useful as a reference material since it was being considered as a support for Fe–Cu catalysts in the work of McDonald et al. [10].

## 3. Results

Fig. 1 shows a TEM image of the primary particles for the precipitated Fe–Cu catalyst precursor. The catalyst, in its as-prepared state, was ultrasonicated beforehand to break up any loose agglomerates. Roughly spherical particles are seen, with an average size of 80 nm. Fig. 2 shows a cumulative mass distribution plot of mass finer (%) vs. equivalent spherical diameter (ESD) for the precipitated Fe–Cu catalyst, as-prepared. Also shown in this plot is the influence of ultrasonic irradiation on the particle size

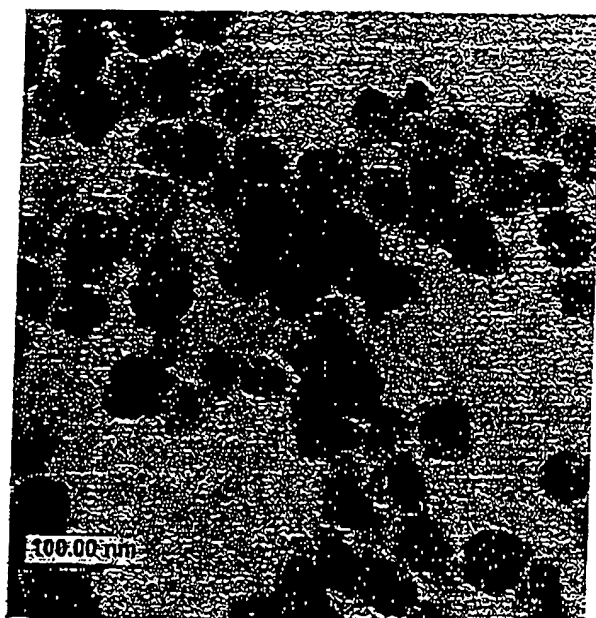


Fig. 1. TEM of a precipitated Fe-Cu catalyst precursor. The catalyst consists of roughly spherical primary particles, with an average particle size of 80 nm.

distribution. This catalyst agglomerate is weak with a broad particle size distribution. Both fracture and erosion occur during ultrasonic fragmentation, and the generation of fine particles below 5  $\mu\text{m}$  may not be acceptable for slurry F-T reactors. Fig. 3 shows a cumulative mass distribution plot for the same catalyst which was spray-dried, but without a binder. Spray-drying improves the attrition resistance of the Fe catalyst, and there is a more uniform particle size distribution. However, ultrasonication causes an increase in the fraction of particles below 5  $\mu\text{m}$ , suggesting that the catalyst is still not resistant to erosion.

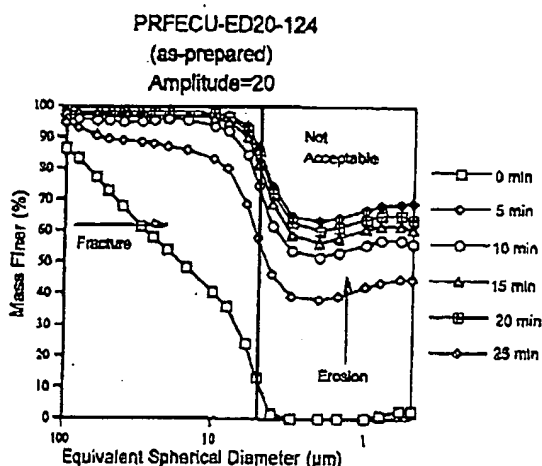


Fig. 2. Sedigraph particle size distribution of a precipitated Fe-Cu catalyst, as-prepared. There is both fracture and erosion of particles after 25 min of ultrasonic fragmentation, indicating that the catalyst is weak. Furthermore, the catalyst has a broad particle size distribution.

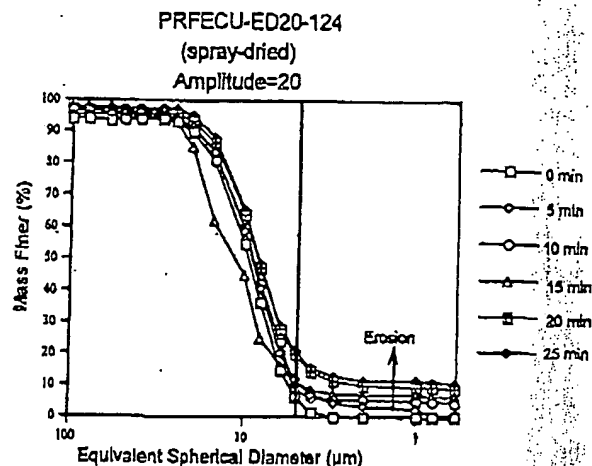


Fig. 3. Sedigraph particle size distribution of a spray-dried precipitated Fe-Cu catalyst. Spray-drying improves the attrition resistance of the catalyst, and there is a more uniform particle size distribution.

Fig. 4 shows a cumulative mass distribution plot for a precipitated Fe-Cu catalyst/potassium silicate mixture that was directly spray-dried. The addition of the  $\text{SiO}_2$  binder further improved the attrition resistance of the catalyst, and now we see little of the fine particles below 5  $\mu\text{m}$  after 25 min of ultrasonic irradiation. The median particle size ( $\approx 8 \mu\text{m}$ ) is smaller than that desired for a commercial F-T process (50–70  $\mu\text{m}$ ); however, this represents a limitation of our bench-top spray dryer. Nevertheless, we have shown that by using a spray-drying technique, we could produce a more attrition-resistant Fe F-T catalyst. Fig. 5 shows an SEM image of the spray-dried agglomerates. Based on the length scale, very few particles bigger than 10  $\mu\text{m}$  are seen in this image. This was traced to a bias in the SEM sampling procedure, which skews the particle size distribu-

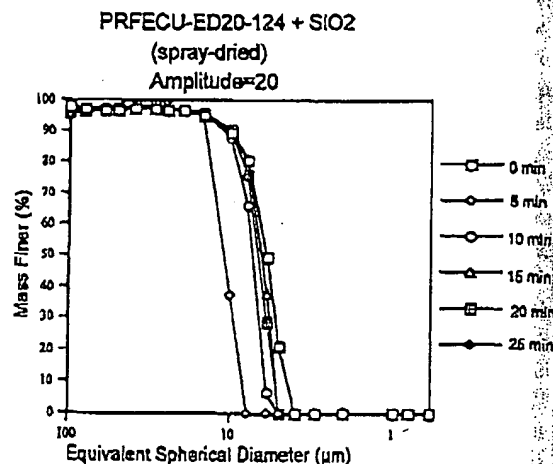


Fig. 4. Sedigraph particle size distribution of a spray-dried precipitated Fe-Cu catalyst containing silica. No erosion below 5  $\mu\text{m}$  has occurred after 25 min of ultrasonic irradiation. Addition of silica further improves its attrition resistance.

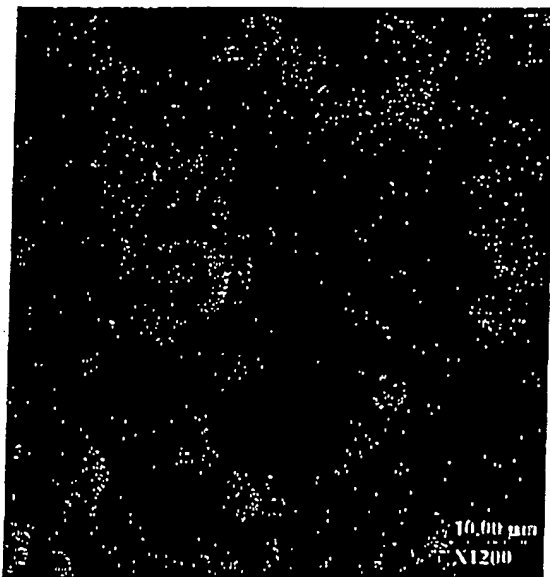


Fig. 5. SEM image of the spray-dried precipitated Fe–Cu catalyst containing silica. The agglomerated particles are roughly spherical, typical for a spray-drying process.

tions to smaller sizes. Smaller particles tend to stick to the carbon tape on the SEM stub more favorably than larger particles. The larger particles are more likely to come off the carbon tape when the SEM stub is shaken to remove excess particles. To verify the presence of larger particles, the catalyst was first sieved using a standard testing sieve having pore openings of 38  $\mu\text{m}$ , and the remaining large particles were used for the SEM analysis. Fig. 6 shows an SEM image of the same catalyst. Large size particles are seen in Fig. 6 that are not seen in Fig. 5. The larger

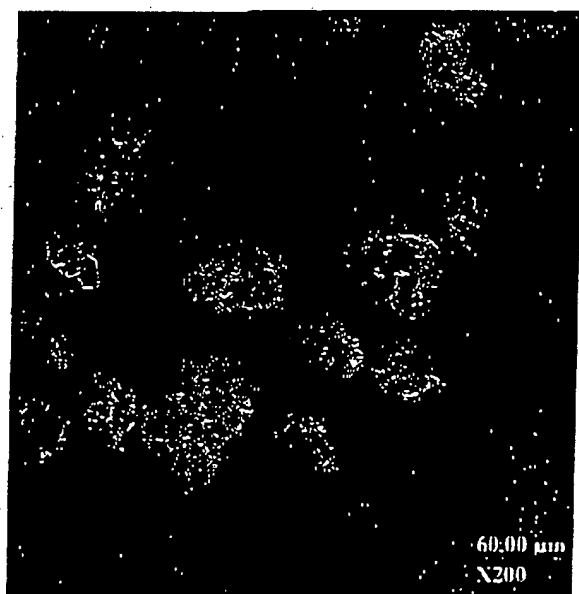


Fig. 6. SEM image of the spray-dried precipitated Fe–Cu catalyst containing silica. Large particles were obtained by sieving with a standard testing sieve having pore openings of 38  $\mu\text{m}$ .

particles in Fig. 6 are less spherical than the smaller particles in Fig. 5, probably due to the limitations of our spray dryer.

The particle size distributions obtained via sedimentation are not easily compared with the SEM images. First, the particles on the carbon tape tend to overlap. It is difficult to determine whether a particle sitting on top of another particle is an individual particle, or part of an agglomerate. Second, in sedimentation theory, non-spherical particles are specified in terms of “ESD”, i.e., the diameter of a sphere that would have the same sedimentation velocity. With the irregular shaped particles seen in the SEM, it is not obvious how the particle size seen in the image can be converted to an ESD. Third, sedigraph particle size analysis samples a large cross-section of the particles, whereas SEM provides localized information. To get good statistics, one would have to count hundreds of particles and also guard against any sampling bias. Hence, we found it best to use the SEM mainly to examine particle morphology.

Fig. 7 shows a cumulative mass distribution plot for a precipitated Fe–Cu catalyst/potassium silicate mixture that was spray-dried and then calcined at 300°C. Fig. 7 is similar to Fig. 4, suggesting that calcination did not appear to significantly improve the strength of the catalyst. Fig. 8 shows an SEM image of the spray-dried/calcined catalyst. These particles have rougher surfaces after calcination than those shown in Fig. 4. The median particle diameter ( $\approx 6 \mu\text{m}$ ) for the spray-dried/calcined catalyst, according to Fig. 7, was smaller than that for the spray-dried catalyst. It is possible that the particles collected after spray-drying were not completely dried. The “wet” particles would lose some water during calcination, shrinking the catalyst particles. Removal of the water present in the catalyst is essential before the Fe F–T catalyst is activated for use in

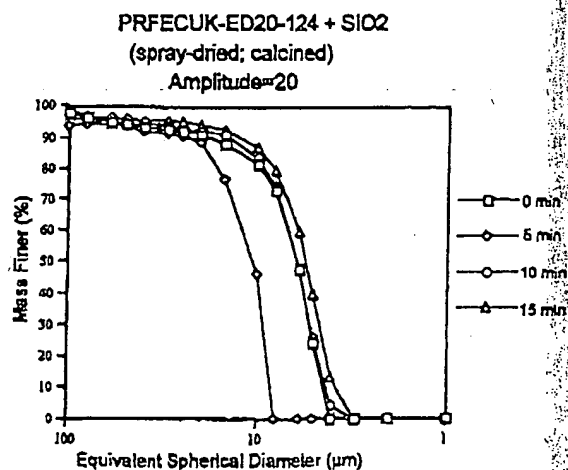


Fig. 7. Sedigraph particle size distribution of a precipitated Fe–Cu catalyst containing silica, which was spray-dried and then calcined at 300°C. The median particle diameter is smaller than that for the spray-dried catalyst.

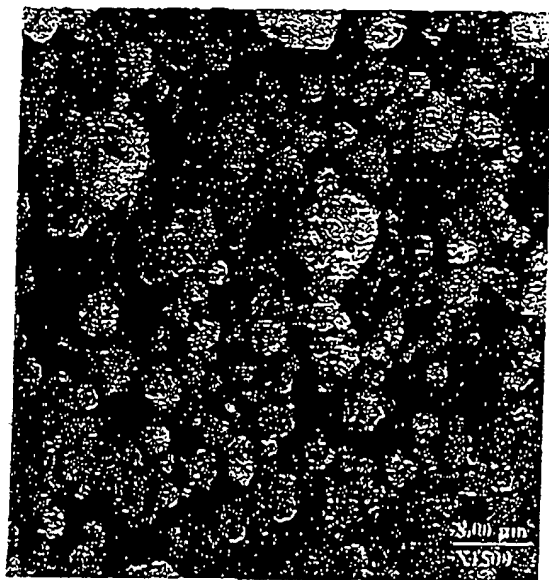


Fig. 8. SEM image of the precipitated Fe-Cu catalyst containing silica, which was spray-dried and then calcined at 300°C. These particles have much rougher surfaces than the spray-dried catalyst particles (Fig. 5).

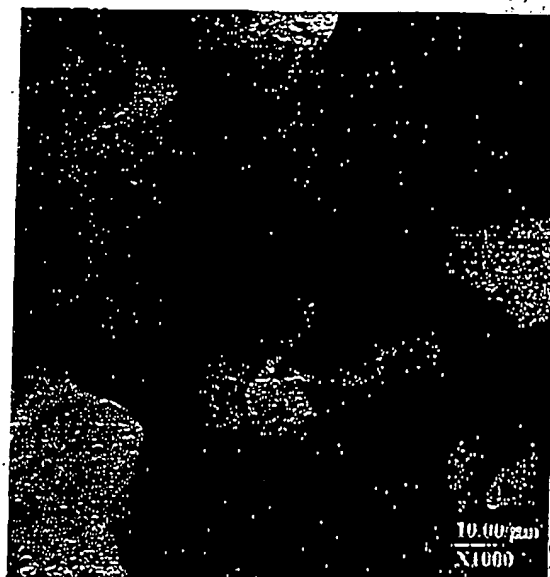


Fig. 10. SEM image of a precipitated Fe-Cu catalyst containing silica, calcined at 300°C before spray-drying. These particles are not spherically shaped, and are larger in size than the spherically shaped spray-dried particles.

a reaction run. However, it is also important that the calcination temperature be low enough that no adverse chemical reactions (formation of interfacial silicate phases) occur between the Fe F-T catalyst and the  $\text{SiO}_2$  support.

Fig. 9 shows a cumulative mass distribution plot for a precipitated Fe-Cu catalyst/potassium silicate mixture that was first calcined at 300°C in its dried state before spray-drying. No erosion occurred below 5  $\mu\text{m}$  after 25 min of ultrasonic irradiation. The median particle diameter ( $\approx 23 \mu\text{m}$ ) for this catalyst is larger than those for the other two synthesized catalysts. The reason is that the catalyst was calcined before being spray-dried. Fig. 10 shows an SEM image of the calcined/spray-dried catalyst. The particles

were irregularly shaped, despite being spray-dried. The irregular shapes must have resulted when the catalyst was first calcined, with the particle shapes being preserved during spray-drying.

Fig. 11 shows a cumulative mass distribution plot for a precipitated Fe-Cu catalyst, which was initially spray-dried, then a potassium silicate solution was added, and the mixture was again spray-dried. The ultrasonic fragmentation technique shows evidence for some erosion, suggesting that  $\text{SiO}_2$  addition after initial spray-drying may not be as effective as the addition before the powder is spray-dried.

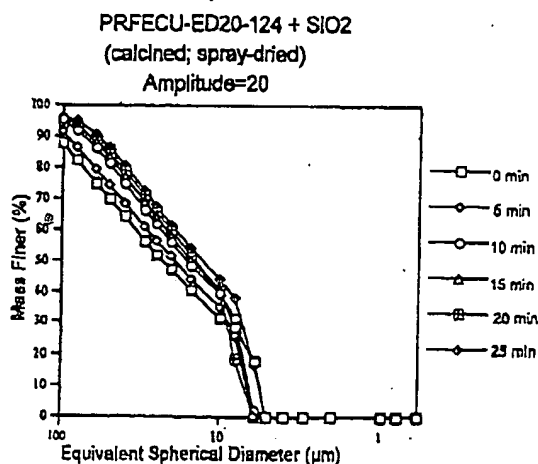


Fig. 9. Sedigraph particle size distribution of a precipitated Fe-Cu catalyst containing silica, calcined at 300°C in its dried state before spray-drying. No erosion below 5  $\mu\text{m}$  has occurred after 25 min of ultrasonic irradiation. Furthermore, the median particle diameter is larger, compared to the other synthesized catalysts.

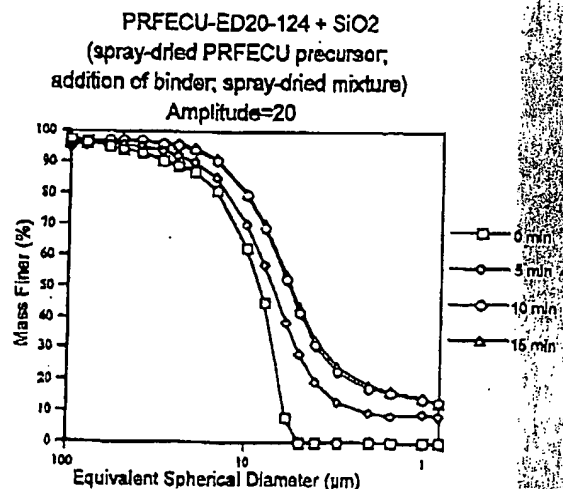


Fig. 11. Sedigraph particle size distribution of a precipitated Fe-Cu catalyst containing silica. The Fe-Cu precursor was first spray-dried before adding silica, and the mixture was again spray-dried. This catalyst is weaker than the other catalysts due to generation of fine particles by erosion.



Fig. 12. SEM image of the precipitated Fe-Cu catalyst containing silica, where the Fe-Cu precursor was first spray-dried before adding silica. These particles look similar to the spray-dried catalyst (Fig. 5).

Fig. 12 shows an SEM image of this catalyst. These particles looked similar to those in the catalyst that was spray-dried after SiO<sub>2</sub> addition (Fig. 5), yet this catalyst was not attrition-resistant to erosion compared to the spray-dried catalyst. It is clear that examination of the external structure alone is not sufficient for determining the strength of the catalyst.

Fig. 13 shows a cumulative mass distribution plot for a VISTA alumina, which was used as a reference sample for comparison with the precipitated Fe F-T catalysts. The median particle diameter ( $\approx 22 \mu\text{m}$ ) is similar to that for the calcined/spray-dried catalyst. However, both the VISTA alumina and the catalyst where silica was added

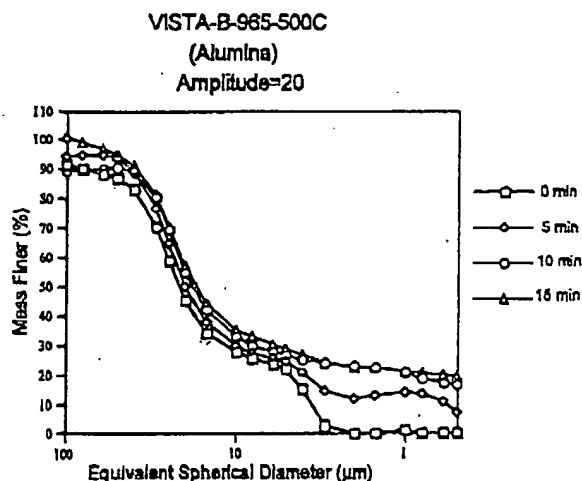


Fig. 13. Sedigraph particle size distribution of VISTA-B-965-500C sample. The starting alumina from VISTA was sieved and calcined in air at 500°C. Very little fracture occurs after 15 min of ultrasonic irradiation, although some erosion has occurred.



Fig. 14. SEM picture of a VISTA alumina. The alumina is non-spherically shaped since it is not spray-dried, and is larger in size than the spherically shaped precipitated Fe F-T catalysts.

after first spray-drying the catalyst precursor (Fig. 11) were weaker than the other prepared catalysts. SEM image (Fig. 14) of the VISTA alumina showed that it consisted of irregularly shaped agglomerates, since this alumina did not come from a spray-drying step. The morphology of the calcined/spray-dried catalyst (Fig. 10) is similar to that of the VISTA alumina; however, the catalyst appears to be more attrition-resistant than the alumina, since it shows no erosion during ultrasonic fragmentation.

#### 4. Discussion

In a previous study, Kalakkad et al. [11] performed an ultrasonic fragmentation test on a commercial iron oxide catalyst, prepared by United Catalyst (UCI), that did not contain a binder. They found that, after 10 min of ultrasonic irradiation at an amplitude of 20, the catalyst broke down completely to the constituent primary particles. Thus, the binderless catalyst agglomerate was extremely weak. Further evidence by SEM [11] confirmed the break up of the catalyst agglomerates after ultrasonic treatment. Datye et al. [12] then performed an ultrasonic fragmentation test on a similar UCI iron oxide catalyst that contained a kaolin binder. They also found that, after ultrasonic treatment at the same amplitude and time, the kaolin-containing catalyst also broke down completely, as confirmed by SEM. It was found that even after 1 min of ultrasonic irradiation at the same amplitude, the kaolin-containing catalyst broke down to the same extent as the binderless catalyst [1].

It was obvious that the kaolin was not very effective as a binder. Analysis by TEM [1,12] on the kaolin-containing

catalyst showed that kaolin and iron oxide catalyst occurred as two distinct phases after ultrasonic treatment. Also, both the kaolin and the iron oxide had a plate-like morphology that was not conducive to creating strong interlocking forces between the primary particles. Since the morphology of the primary particles as well as the binder play an important role in controlling agglomerate strength, we felt it was necessary to explore other morphologies to provide improved attrition resistance in these Fe F-T catalyst particles. Pietsch [13] has provided an excellent overview of the various binding mechanisms which may play a role in agglomerate strength. These mechanisms include sinter bridges, chemical reactions, liquid bridges which may harden to form solid bridges, electrostatic forces, interlocking forces, and capillary forces.

For this work, we chose silica as a binder because precipitated silica provides very irregular structures that should be more conducive to creating interlocking forces to hold the Fe F-T catalyst together. In the initial experiments, we used the primary particles from the plate-like UCI catalyst and added potassium silicate solution followed by precipitation of the silica. There was a slight improvement in catalyst strength as measured from ultrasonic fragmentation. Changing the morphology of the primary particles from plate-like to that of the precipitated Fe-Cu catalysts used in this study (Fig. 1) we see a significant improvement in the strength of this catalyst. Therefore, we conclude that the shape of the primary iron oxide precursor particles is important in determining the attrition resistance of the Fe F-T catalysts.

When the slurry consisting of the precipitated Fe-Cu catalyst and potassium silicate was spray-dried, there was a further improvement in catalyst strength. In these experiments, the slurry was first subjected to ultrasonication to break up any loose agglomerates before running into the spray dryer. This is to avoid feeding larger particles to the spray dryer, which, it has been suggested [13], should be used only if an adequate amount of binder is present or there are sufficient number of small particles. When we examine the strength of the spray-dried precipitated Fe-Cu catalyst without any addition of silica binder, we find that the agglomerates are still not strong enough for the slurry reactor application. It is clear that particle morphology helps, but is not sufficient to make strong agglomerates.

In the next series of experiments, we investigated various approaches for adding silica to the catalyst precursor. The silica was added either before or after spray-drying, and the role of a calcination step was also explored. It was found that the addition of silica after first spray-drying was not effective in imparting attrition resistance to the catalyst agglomerates. Furthermore, calcination did not significantly improve the strength of the spray-dried catalyst. However, when calcination was performed before the spray-drying step, irregular shaped agglomerates were formed. The calcined/spray-dried catalyst particles were

Table 1  
BET surface area of the precipitated Fe F-T catalysts

Sample	Bet surface area (m <sup>2</sup> /g)
PRFECU-ED20-124 + SiO <sub>2</sub> (calcined; spray-dried)	224.3
PRFECU-ED20-124 + SiO <sub>2</sub> (spray-dried)	127.5
PRFECU-ED20-124 + SiO <sub>2</sub> (spray-dried; calcined)	158.7
PRFECU-ED20-124 + SiO <sub>2</sub> (spray-dried)	
PRFECU precursor; addition of binder; spray-dried mixture	81.3

non-spherical, yet they exhibited superior attrition resistance. The shape of the catalyst particles may be important for proper slurry hydrodynamics in a bubble column reactor. Furthermore, we expect that during operation of stirred tank reactor, more erosion would be seen with non-spherical particles than with smooth, spherical particles.

Another parameter that is important in these catalysts is the surface area. Powders with high surface areas would generally be preferred since the reaction takes place at the gas-solid interface. Table 1 gives surface areas for the precipitated Fe F-T catalysts, using a BET N<sub>2</sub> adsorption analyzer. Of the precipitated catalysts, the calcined/spray-dried catalyst had the highest surface area while the lowest surface area was seen in the catalyst where silica was added after initial spray-drying of the catalyst precursor. We suspect that the silica added after spray-drying tends to block access to the interior pores, causing the drop in surface area. In the case of these iron oxide catalysts, it is known that they have to be first transformed into reduced iron phases, such as iron carbide, which is the active phase for this reaction [14]. The phase transformations accompanying catalyst activation result in a chemical attrition of the catalyst [11], which needs to be considered when determining the attrition resistance of these catalysts. We have also performed cross-section TEM for studying the particle-binder interactions, and to map the internal structure of the catalyst agglomerates. These results will be described elsewhere [15].

## 5. Summary

The precipitated Fe-Cu catalyst, as-prepared, was weak compared to the same catalyst which was spray-dried. Spray-drying improved the attrition resistance of the Fe F-T catalyst. The role of silica binder addition and calcination was explored to increase the attrition resistance of these catalysts. The precipitated catalysts were compared to a VISTA alumina, which was used as a reference sample. Ultrasonic fragmentation followed by particle size distribution measurements were used to characterize the strength of these catalyst agglomerates. It was found that the precipitated Fe-Cu catalyst that was spray-dried but

had no added  $\text{SiO}_2$  was comparable in strength to the alumina reference material, but both were weaker than the spray-dried, calcined/spray-dried and spray-dried/calcined catalysts. Calcination of the catalyst after spray-drying did not impart any additional strength to the catalyst. We conclude that particle morphology is an important parameter determining the strength of spray-dried agglomerates. In this study, the precipitated silica was found to provide a morphology that is suitable for holding together the primary catalyst particles. Further tests of attrition behavior will require the use of reactor tests which will be the subject of future work.

### Acknowledgements

The authors would like to thank the US Department of Energy and the Federal Energy Technology Center (FETC) under contract numbers DE-FG-22-95PC95210 and DE-FG26-98FT40110 for their financial support of this project.

### References

- [1] H.N. Pham, J. Reardon, A.K. Darcy, *Powder Technol.* 103 (1999) 95.
- [2] R. Oukaci, A.H. Singleton, D. Wei, J.G. Goodwin Jr., Symposium on Syngas Conversion to Fuels and Chemicals, Division of Petroleum Chemistry, 217th National Meeting, March 21–25, 1999, American Chemical Society, Anaheim, CA, Vol. 44, pp. 91–92.
- [3] S.G. Thoma, M. Ciftcioglu, D.M. Smith, *Powder Technol.* 58 (1991) 53.
- [4] S.G. Thoma, M. Ciftcioglu, D.M. Smith, *Powder Technol.* 68 (1991) 71.
- [5] L. Nikolic, L. Radonjic, *Thin Solid Films* 295 (1997) 101.
- [6] C.J. Brinker, J.G.W. Scherer, *Sol-Gel Science, The Physics and Chemistry of Sol-Gel Processing*, Academic Press, Boston, 1990.
- [7] H.E. Bergna, Attrition-resistant porous particles produced by spray drying, *ACS Symp. Ser.* (411) (1989) 55–64.
- [8] E. Horisawa, A. Komura, K. Danjo, A. Otsuka, *Chem. Pharm. Bull.* 43 (1995) 488.
- [9] D. Bortzmeyer, J.C. Goinard, *Powder Technol.* 86 (1996) 163.
- [10] M.A. McDonald, R.J. Gormely, M.F. Zarochak, M.F., Estimation of surface site density on iron Fischer-Tropsch catalyst by means of a test reaction, *Proceedings of the 1997 Coal Liquefaction and Solid Fuels Contractors Review Conference*, Pittsburgh, PA.
- [11] D.S. Kalakkad, M.D. Shroff, S. Kohler, N. Jackson, A.K. Darcy, *Appl. Catal.* 133 (1995) 335.
- [12] A.K. Darcy, M.D. Shroff, Y. Jin, R.P. Brooks, J.A. Wilder, M.S. Harrington, A.G. Sault, N.B. Jackson, *Stud. Surf. Sci. Catal.* 101 (1996) 1421.
- [13] W. Pietsch, *Chem. Eng. Prog.* 92 (1996) 29.
- [14] M.D. Shroff, D.S. Kalakkad, K.E. Coulter, S.D. Kohler, M.S. Harrington, N.B. Jackson, A.G. Sault, A.K. Darcy, *J. Catal.* 156 (1995) 185.
- [15] H.N. Pham, A.K. Darcy, The synthesis of attrition-resistant slurry phase Iron Fischer-Tropsch catalysts, *Catal. Today*, submitted for publication.



**This Page is Inserted by IFW Indexing and Scanning  
Operations and is not part of the Official Record**

**BEST AVAILABLE IMAGES**

Defective images within this document are accurate representations of the original documents submitted by the applicant.

Defects in the images include but are not limited to the items checked:

- ☐ BLACK BORDERS
- ☐ IMAGE CUT OFF AT TOP, BOTTOM OR SIDES
- ☐ FADED TEXT OR DRAWING
- ☐ BLURRED OR ILLEGIBLE TEXT OR DRAWING
- ☐ SKEWED/SLANTED IMAGES
- ☒ COLOR OR BLACK AND WHITE PHOTOGRAPHS
- ☐ GRAY SCALE DOCUMENTS
- ☐ LINES OR MARKS ON ORIGINAL DOCUMENT
- ☐ REFERENCE(S) OR EXHIBIT(S) SUBMITTED ARE POOR QUALITY
- ☐ OTHER: \_\_\_\_\_

**IMAGES ARE BEST AVAILABLE COPY.**

**As rescanning these documents will not correct the image problems checked, please do not report these problems to the IFW Image Problem Mailbox.**